Received: 28 May 2021 | Revised: 22 August 2021 | Accepted: 23 August 2021

DOI: 10.1002/app.51612

ARTICLE

Applied Polymer SCIENCE WILEY

Investigation into poloxamer 188-based cubosomes as a polymeric carrier for poor water-soluble actives

Swanya Yakaew[1] | **Kunlathida Luangpradikun**[1] | **Preeyawass Phimnuan**[1] | **Nitra Nuengchamnong**[2] | **Nuntaporn Kamonsutthipaijit**[3] | **Supagorn Rugmai**[3] | **Wongnapa Nakyai**[4] | **Sukunya Ross**[5] | **Malyn Ungsurungsei**[6] | **Jarupa Viyoch**[1] | **Gareth Ross**[5]

[1]Department of Pharmaceutical Technology, Faculty of Pharmaceutical Sciences and Center of Excellence for Innovation in Chemistry, Naresuan University, Phitsanulok, Thailand

[2]Science Laboratory Center, Faculty of Science, Naresuan University, Phitsanulok, Thailand

[3]Synchrotron Light Research Institute (Public Organization), Nakhon Ratchasima, Thailand

[4]Department of Chemistry, Faculty of Science, Ramkhamhaeng University, Bangkok, Thailand

[5]Department of Chemistry, Faculty of Science, Naresuan University, Phitsanulok, Thailand

[6]Research & Development Division, S & J International Enterprises Public Company Limited, Bangkok, Thailand

Correspondence
Jarupa Viyoch, Department of Pharmaceutical Technology, Faculty of Pharmaceutical Sciences and Center of Excellence for Innovation in Chemistry, Naresuan University, Phitsanulok 65000, Thailand.
Email: jarupav@nu.ac.th

Gareth Ross, Department of Chemistry, Faculty of Science, Naresuan University, Phitsanulok 65000, Thailand.
Email: gareth@nu.ac.th

Funding information
S&J International Enterprises Public Company Limited; Newton Fund PhD, Grant/Award Number: 351290033; Research and Researchers for Industries Grants (RRI), Grant/Award Number: PHD57I0030

Abstract

Cubosomes and other lyotropic liquid crystal (LLC) phases are of great interest in many fields due to their potential as delivery systems. This study prepared poloxamer 188 (Pluronic® F68 [F68]) based cubosomes utilizing a low energy method and reports LLC structure stability, rheological behavior and carrier properties of the formed cubosomes. Mixtures of F68 and water were investigated and showed a concentration dependent viscoelastic behavior, ranging from a viscous liquid (30% F68) to hard gels (70% F68). Small-angle X-ray scattering showed cubosomes (Im3m) were present at F68 concentrations between 45% and 60%. Cubosomes fabricated from 50% F68 and 50% water were selected as the best composition and gave stable cubic structures for at least 10 months without additional stabilizing agent. To assess the use with poor water-soluble molecules, artocarpin (AR) was added to the F68-based cubosome. The developed cubosome possessed enhanced AR solubility due to the high affinity to the hydrophobic regions present in the cubic formation. Furthermore, an in vitro permeation study showed faster permeation rates of the developed cubosomes when compared to a cream-based formulation. Collectively, these findings demonstrate that the F68-based cubosomes represent a promising low-cost active carrier for enhancing the solubility and permeability of low water-soluble molecules.

KEYWORDS
drug delivery systems, gels, liquid crystals, rheology, surfactants

1 | INTRODUCTION

The incorporation and subsequent delivery of poor water-soluble active ingredients remain one of the most challenging aspects of cosmetic and drug formulation development.[1–3] For example, more than 40% of pharmaceutical compounds are considered to have poor water solubility. Thus, there is a great need for smart formulation approaches to help overcome this challenge such as lyotropic liquid crystal (LLC), lipid nanoparticles and solid dispersions. Among these the self-assembly of block copolymers to LLC has attracted considerable attention in both the scientific and industrial fields.[4–6] There are a number of different LLC structures available such as, lamellar, hexagonal, bicontinuous cubic and cubic micelles.

This works focal point is bicontinuous cubic LLCs often referred to as cubosomes, which continue to garner interest from researchers due to their potential for use as delivery systems.[7–9] Cubosomes consist of aqueous channels and lipid bilayer membranes within their three-dimensional (3D) structure. They possess promising advantages for delivery systems as they can be loaded with both hydrophilic and hydrophobic drugs, leading to pronounced increases in solubility, stability, bioavailability as well as protecting encapsulated molecules.[10–12] The term cubosome covers three different liquid crystal (LC) structures; diamond (D, Pn3m), primitive (P, Im3m), and gyroid (G, Ia3d). To help determine which LC is present methods such as small angle X-ray scattering (SAXS) are commonly used and LC is by defined the spacing ratios.[13,14]

The majority reported cubosomes are prepared from the lipid monoolein (MO), (at high purity ~99%). There are however, three major obstacles to widespread use of MO-based cubosomes. MO, generally requires the use of high energy formation methods that require specific equipment to form the cubic phases, leading to higher cost of production, such as sonication and high-pressure homogenizer.[15] Moreover, MO-based cubosomes need a stabilizing agent, a typical stabilizer is poloxamer 407 (Pluronic® F127 [F127]). F127 is an excellent steric stabilizer that can often be used to prevent particle aggregation for extended periods of time.[16] All of these factors mean that the use of MO and other lipids result in significantly higher costs when compare to others amphiphilic molecules.

The poloxamers or Pluronics® are a family of triblock amphiphilic block copolymers.[17] These nonionic triblock copolymers are composed of the type poly(ethylene oxide)-b-poly(propylene oxide)-b-poly (ethylene oxide) (PEO-PPO-PEO). Numerous interesting LLC can be formed depending on block copolymer concentration, composition (PPO/PEO ratio), solvent conditions, and the presence of additives.[18,19] A wide range of commercial PEO-PPO block sizes are available, PEOn-PPOm-PEOn, where n and m represent the number of PEO and PPO units, respectively. In addition to F127 being used as a stabilizer with MO, blends of F127 with Poloxamer 188 or Pluronic® F68 LF Pastille (F68) have been used to encapsulate Ropivacaine,[20] ketorolac tromethamine,[21] and GM1,[22] nanocomplexes of chitosan or hydroxypropylmethyl cellulose (HPMC) loaded into F127/F68 hydrogels for the delivery of heparin (used for pulmonary embolism, deep vein thrombosis).[23] Poloxamer 188, has the block composition of $PEO_{76}PPO_{30}PEO_{76}$ with an average molecular weight ~8400. F68 has been widely use in cosmetic and pharmaceutical as solubilizer, thickener and gelling agent. However, single use of F68 as a carrier is absent from the literature.

Therefore, the aim of this study is to develop a F68-based LLC system as a model carrier for poor water-soluble molecules, a schematic representation of the proposed system is depicted in Figure 1. The use of a single component allows for a simple cost-effective approach in terms of both the material and preparation method. The optimum conditions for F68-based LLC systems using a low energy stirring technique were investigated. In order to further test the developed system, a model poor-water soluble molecule was selected. The model molecule for this work was artocarpin (AR), which is the major compound of *Artocarpus incisus* (breadfruit), this compound presents biological activities such as antioxidant activity,[24] melanogenesis-inhibition,[25] restoration of wrinkled-skin fibroblast activities[26] and anticancer activity.[27] However, a drawback of this molecule is its poor water solubility with a partition coefficient (log P) of 5.18. The fabricated F68-based LLC systems were evaluated in terms of their structure, morphology, stability, and rheology behavior. We also assessed the in-vitro permeation properties of the developed AR contains F68-based LLC systems.

2 | MATERIALS AND METHODS

Poloxamer 188 (Pluronic® F68 LF Pastille [$PEO_{76}PPO_{30}PEO_{76}$]) with an average molecular weight around 8400 g/mol and poloxamer 407 (Pluronic® F127 [$PEO_{101}PPO_{56}PEO_{101}$]) with an average molecular weight around 12,600 g/mol was purchased from BASF (Bradford, UK). Methanol (≥98% purity) and HPLC water grade were purchased from RCL Labscan (Bangkok, Thailand). Strat-M® was purchased from EMD Millipore (Danvers, MA).

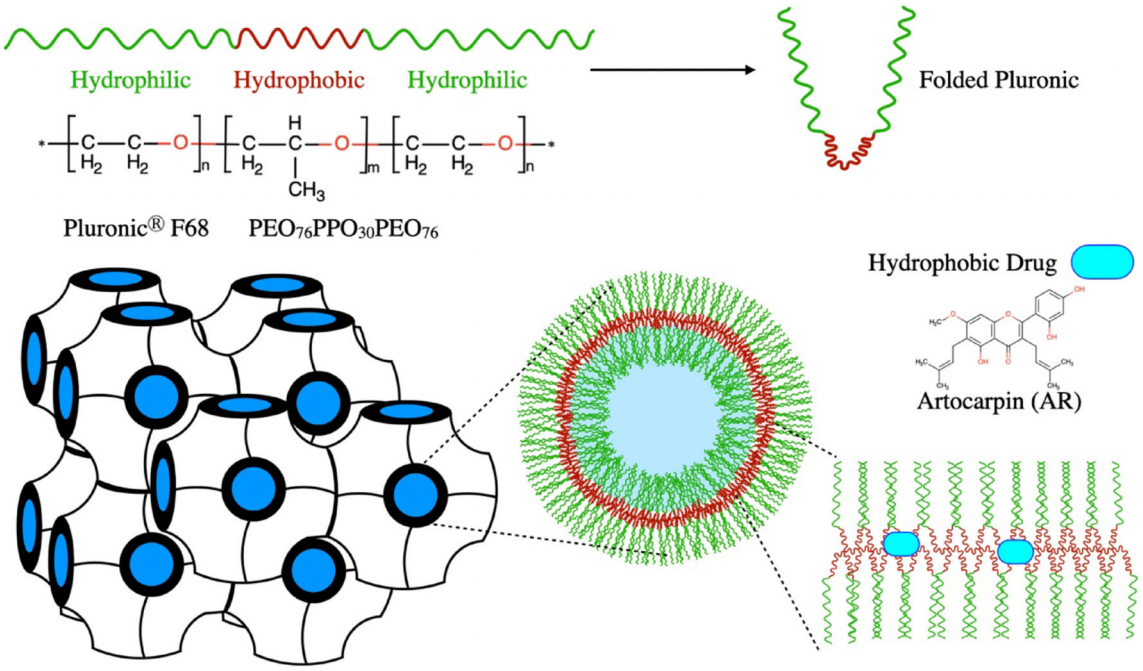

FIGURE 1 Schematic representation of the proposed cubosome carrier system [Color figure can be viewed at wileyonlinelibrary.com]

2.1 | Preparation of the AR-enriched extract

Fresh heartwood of *A. altilis* (Parkinson ex F.A.Zorn) Fosberg was collected in Phitsanulok province, Thailand, and recorded as kew-2653919. The plant was identified by Dr. Pranee Nangngam, and a specimen voucher (PNU no. 003511) was deposited at the PNU Herbarium of the Faculty of Sciences at Naresuan University. The AR-enriched extract of *A. altilis* heartwood was prepared according to the method previously described.[28,29] Briefly, the heartwood was cut into small pieces and dried in a hot-air oven for 3 days at 45°C. Then the dried heartwood was covered and macerated with diethyl ether at room temperature for two cycles (2 days per cycle). The pooled ether extract was filtered and concentrated using rotary evaporation and the AR-enriched extract was obtained using column chromatography. The column packed with silica gel (No. 60; Merck, Darmstadt, Germany) was loaded with the ether extract and filled to the top with the eluting solvent, hexane, which continuously flowed through the column. The extract was then eluted with increasing concentrations of ethyl acetate and collected in 5 ml fractions. The presence of flavonoid compounds in each fraction was evaluated using thin-layer chromatography (TLC) (Merck, Darmstadt, Germany). Fractions exhibiting similar TLC profiles were pooled and concentrated by rotary evaporation. The obtained extract was stored at 4°C before use.

2.2 | Quantification of AR in the AR-enriched extract

AR content in the extract was determined using isocratic high performance liquid chromatography (HPLC, SPD-20A UV detector and LC-20AP pump, Shimadzu Co., Ltd., Kyoto, Japan) with a 250 × 4.60 mm^2 diameter column packed with 5 mm C18 (Phenomenex Gemini column). The mobile phase consisted of methanol and water (80:20). The extract was dissolved in the mobile phase and filtered through a 0.45 mm nylon filter. The analysis was carried out in isocratic mode at a flow rate of 1 ml/min. The volume injected was 20 ml and monitored at a wavelength of 282 nm. The amount of AR was calculated by integrating the peak using a calibration curve generated from standard AR obtained from a previous study.[29] All experiments were performed in triplicate (n = 3), and all mobile phases were of HPLC grade.

2.3 | Preparation of F68-based cubosomes

Cubosomes of F68 and water at different weight ratios were prepared using a modified low energy stirring method that is similar to a previously reported method.[30] Briefly, 30–70%wt/wt F68 was mixed with DI water to make the final volume of 100%wt/wt. This solution was then continuously stirred until a homogeneous mixture was obtained. The samples were then allowed to reach

equilibrium at ambient temperature for a minimum of 3 days (up-to 14 days).

2.4 | Preparation of AR loaded cubosomes

AR-loaded cubosomes were prepared at the selected ratio of 1:1 (F68/water) based on a modified version of the method reported by Eblovi et al.[31] First, the F68 and AR (1% wt/wt) were accurately weighed and dissolved/blended with the required volume of water. Then continuously stirred to achieve a homogeneous state and again allowed to reach equilibration for 3 days at room temperature to fully develop the cubic phases.

2.5 | Small-angle X-ray scattering

The SAXS measurements were performed on beamline 1.3 W: SAXS/WAXS at the Synchrotron Light Research Institute (Public Organization), Thailand. Each sample was applied to the stainless-steel frame with Kapton windows. They were then exposed to X-rays (9 keV) at room temperature for 5 min with the sample-to-detector distance of 1600 mm. The q-range used was 0.01–0.5 nm^{-1} (scattering vector $q = 4\pi\sin[\theta]/\lambda$, where θ is the scattering angle and λ is the wavelength). Silver behenate was used as a standard for the calibration. The raw SAXS data was processed using the SAXSIT program, which is developed in-house to obtain the 1D scattering curve, which plots intensity versus q-value. This scattering curve enables the identification of peak positions, and their correlation with Miller indices, to identify the different liquid crystalline structures and space groups for the dominant internal nanostructure of the sample. The SAXSIT software was also used for this analysis.

The interlayer spacing of the LC phases (d) was determined from the Bragg peaks obtained for each sample, using q, which corresponds to the position of each reflection following Equation (1):

$$d = 2\pi/q \quad (1)$$

In the case of the cubic phase, the lattice parameter (a) was calculated with the most intense reflection as follows:

$$a = \left(h^2 + k^2 + l^2\right)^{1/2} d \quad (2)$$

where h, k, and l are the Miller indices. The lattice parameter is also equal to the slope in the indexing of the peaks when plotting between d^{-1} and $(h^2 + k^2 + l^2)^{½}$.[32]

2.6 | Rheological measurements

A rotational rheometer (ARES G2 TA Instruments) was used to measure the viscoelastic properties of the prepared F68-water mixtures. Each sample was place in between two 8 mm serrated-parallel plates with all tests being carried out at 25°C. The top plate was lowered until the sample was in contact with both plates, with a gap of ~1 mm, then the test parameters began. Two test parameters were used for each sample, a frequency sweep from 0.1 to 50 Hz with 0.1% constant strain, and a strain sweep from 0.01% to 150% at a constant frequency of 1 Hz.

2.7 | Particle size distribution

Particle size and particle size distribution were determined by dynamic light scattering (DLS) using a Zetasizer Ultra (Malvern Instruments Ltd., Worcestershire, UK) at 10X dilution of the samples in particle-free purified water. The mean z-average diameter and polydispersity indices (PDI) were obtained by cumulate analysis using the MALVERN software. Each sample was measured in triplicate, with a detector angle of 173° at 25°C.

2.8 | Field emission scanning electron microscopy study

The morphologies of the samples was studied by using FE-SEM (Apreo S, Thermoscientific, MA) samples were analyzed at magnifications of 10,000× and 80,000× with an operating voltage of 10 kV. The cubosome sample were prepared by using diluting the formed stable cubosomes samples (10× dilution) and then pasting onto a glass slide cover before drying overnight at 50°C.

2.9 | In vitro study on penetration of AR loaded cubosome

A synthetic membrane (Strat-M®) was used to mimic human skin. The skin penetration studies were performed using a vertical Franz diffusion cell (Logan Instruments Corp., Model FDC-6 T Diffusion Cell, NJ) with an effective diffusion area of 4.15 cm^2. The receiver chamber was filled with 2% span 20 (Sorbitan monolaurate) in PBS (phosphate-buffered saline, pH 7.4) solution for 8 ml. The chamber was maintained at 37 ± 1°C and continuously stirred at 600 rpm throughout the experiments. 1 ml of the AR loaded cubosomes and AR containing conventional cream (ingredients water, wax and 5% emulsifier; glyceryl stearate and PEG-100

stearate) were compared by adding to the donor compartment covering the membrane surface. An aliquot (200 µl) was withdrawn from the receiver chamber at fixed time intervals (1, 2, 3, 4, 8, 12, 16, and 24 h) with the same volume of fresh receiver solution being added to keep a constant volume. Finally, the penetrant concentration in the receiver chamber was determined by HPLC.

2.10 | Calculation of membrane permeation parameters

The cumulative amount of AR permeated through membrane was plotted as a function of time. The permeation rate of AR at steady state (Js, µg/cm^2 per h) through the membrane was calculated from the slope of linear portion of the cumulative amount permeated through the membrane per unit area versus time plot.[33]

3 | RESULTS AND DISCUSSION

The overarching aim of this work was to investigate a simple but effect method for improving the solubility of poor-water soluble molecules. In order to investigate the equilibrium period, we monitored the self-assembly process of the F68 by SAXS intensities recorded as a function of time (days), the results are presented in Figure 2. After the addition of water to the F68 mixtures for 24 h (day 1), the sample quickly constructs the initial phase with the peak ratios √2:√4 indicating cubic structure as the first phases formed. During the period between day 1 and day 2, the sample registered a slow transfer to equilibration of the P-type cubosome pattern. At day 3, the scattering is characteristic for the P-type cubosome pattern with sharp interface at ratios √2:√4:√6 indicated the equilibrium period of the system. Therefore, the F68-water mixtures were prepared and kept for a minimum of 7 days before further characterization.

3.1 | Investigation and characterization of the effect of F68 concentration of cubosome formation

The next step investigated how the concentration of F68 in water impacts the appearance of the mixtures and how this is related to the viscoelastic behavior of the mixtures. As the concentration of F68 increases, the system transitions from a liquid to a solid phase. The appearance below 40% F68, presented as liquid, with low viscosity. When the concentration passes 40%, the mixture

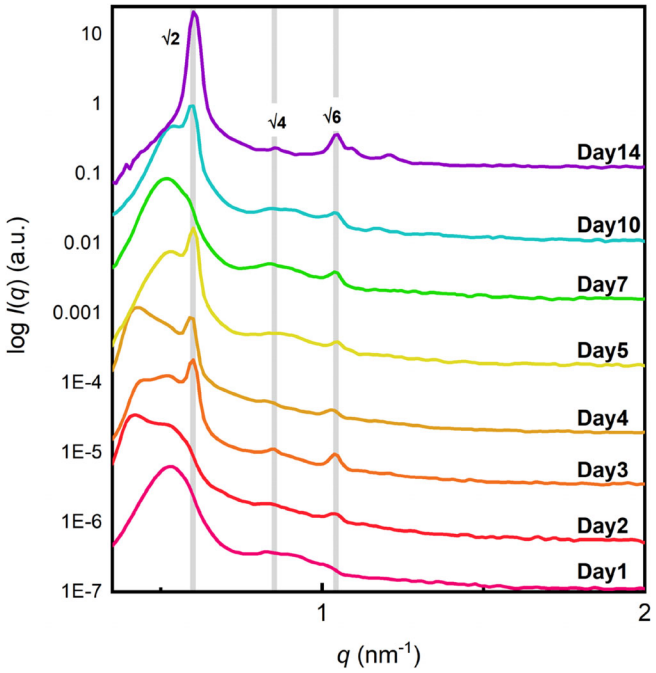

FIGURE 2 Small angle X-ray scattering diffractogram with Bragg peaks and peak assignment for equilibrium period, the self-assembly of F68 recorded as a function of time (days) [Color figure can be viewed at wileyonlinelibrary.com]

becomes a viscous soft gel and upon further increase in F68 concentration the mixtures become a hard gel at ~60%. The appearance at the two most extreme variations in F68 samples are shown photographs in Figure 3, with the 30% F68 (liquid) and 65% F68 (hard gel). This transition can also be thought of as a continuum of viscoelastic behavior. Therefore, to fully analyze this behavior the rheology of samples ranging from 35% to 70% were assessed. The results are also presented in Figure 3, with the storage (elastic) modulus (G′) plotted against frequency and show distinct regions that correspond to the physical appearance of each composition. For the F68-water mixture at 35% F68, the lowest G′ (G′ < 10^3 Pa) value is obtained, due to the sample possessing no ordered structures. At F68 concentrations of 40% and 45%, there is large jump in the G′ (G′ < 10^4 Pa), at these concentrations the mixtures G′ is still dependent on the frequency, with G′ increasing as frequency increases. Although, the G′ is larger than the previous sample it is still less than the value deemed an elastic solid (G′ < 10^4 Pa), thus, the samples appearance is that of a soft gel at this F68 concentration range (40%–45%). When the F68-water concentration is greater than 60%, the G′ of the mixtures is greater than 10^4 Pa (G′ > 10^4 Pa) and the G′ is fully independent of frequency, thus confirming that the F68-water mixtures are hard gels.

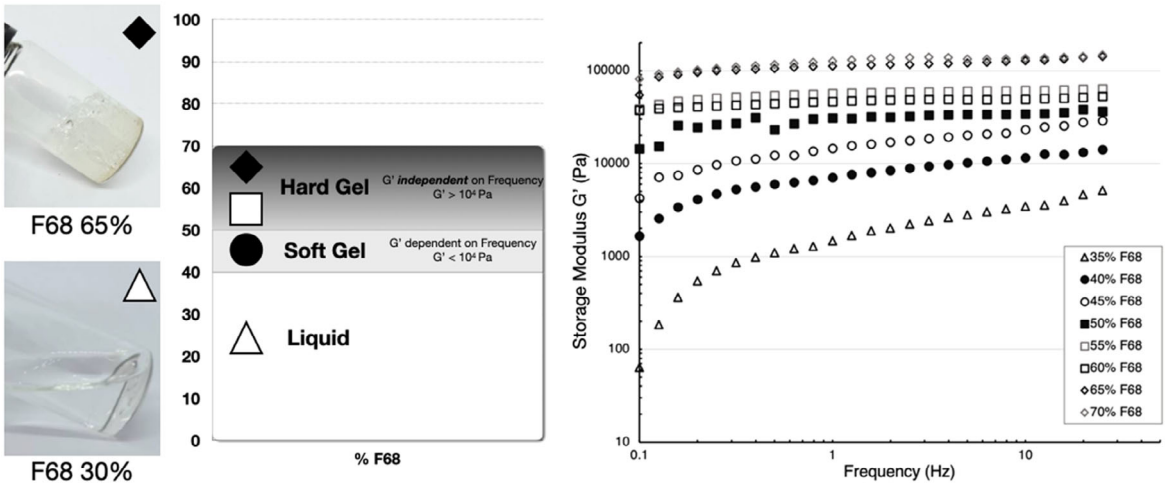

FIGURE 3 Visualization and viscoelastic properties (storage (elastic) modulus vs. frequency) of F68-water mixtures [Color figure can be viewed at wileyonlinelibrary.com]

TABLE 1 Relationship between cubic LLC structures and Bragg peak ratios

LLC structure	Peak ratio
Cubic micellar (fcc)	√3:√4:√8:√11,...
Bicontinuous cubic (Im3m)	√2:√4:√6:√8,...
Bicontinuous cubic (Pn3m)	√2:√3:√4:√6:,..
Bicontinuous cubic (la3d)	√6:√8:√14:√16:,...

Note: Ref. 27.

TABLE 2 Ratio of F68:water, peak position ratios, corresponding structure of LLC phases and lattice parameters

Ratio of F68:water	Peak position ratio	Group spacing	Lattice parameter
45:55	√2:√4:√6	Im3m	14.819
50:50	√2:√4:√6	Im3m	14.747
55:45	√2:√4:√6	Im3m	14.431
60:40	√2:√4:√6	Im3m	14.539
65:35	√3:√8	Fd3m	18.130
70:30	√2:√6:√8	P6mm	8.479

The visualization and rheology data clearly demonstrate that the F68-water mixtures alter as the concentration of F68 is increased. However, to fully define the underlying macro-structures responsible for this the F68-water mixtures from 30% to 70% were analyzed using SAXS. Table 1 presents the different cubic LLC structures and the peak ratios that can be determined from SAXS. 2-dimensional SAXS patterns for the four different patterns found are shown in Figure 4(a), these correspond to no liquid crystalline phase, bicontinuous cubic (Im3m), micellar cubic (Fd3m) and (P6mm) at 30%, 45%, 65%, and 70%, respectively.

From the SAXS diffractogram presented in Figure 4 (b), the 1D plots show that samples containing 40% and lower of F68 give no liquid crystalline phases. The formation of liquid crystalline regions requires at least 45% of polymer to form liquid crystalline phases, which exists as a soft viscous gel. These peaks were observed with relative positions at ratios √2:√4:√6 and are in accordance with the bicontinuous cubic phase structure with Im3m group spacing, indicating cubosomes with a primitive type cubic nanostructure (P-type). The cubic phase is stable between 45% and 60% of polymer concentration. The system also yields a Fd3m, a spinel-type crystal structure at 65% of the polymer as relative positions at ratios √3:√8. As the concentration of polymer further increases to 70%, the peak ratio of √2:√6:√8 is found which represent the P6mm group spacing. The peaks allow the different phases to be determined, the sequence of phases with increasing F68 concentration is Im3m cubic to Fd3m, micellar cubic phase then P6mm. Table 2 provides a summary of the results and shows the ratio of F68:water and the corresponding peak position ratios, group spacings and lattice parameters.

3.2 | Detailed cubosome characterization of 50% F68-water mixture system

From Figures 3 and 4, cubic structures are present between F68 contents of 45%–65%. When looking at the

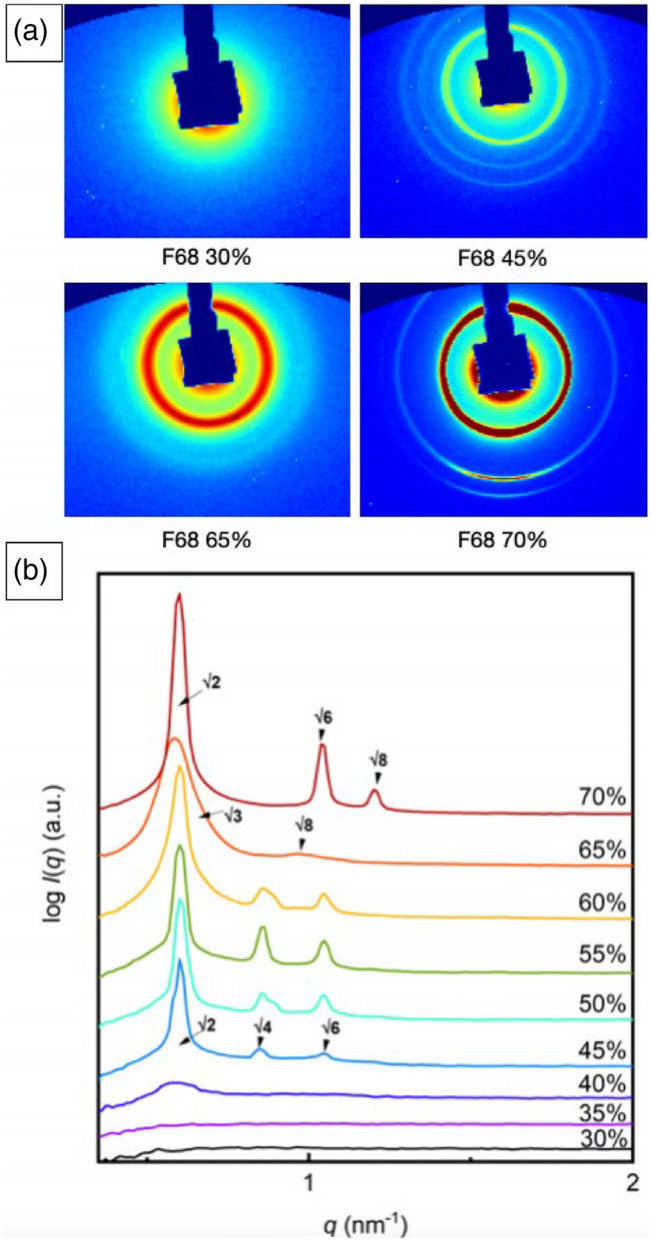

FIGURE 4 (a) 2D small angle X-ray scattering patterns for F68 concentrations ranging from 30% to 70%. (b) Small angle X-ray scattering diffractogram with Bragg peaks and peak assignment for F68 concentrations ranging from 30% to 70% [Color figure can be viewed at wileyonlinelibrary.com]

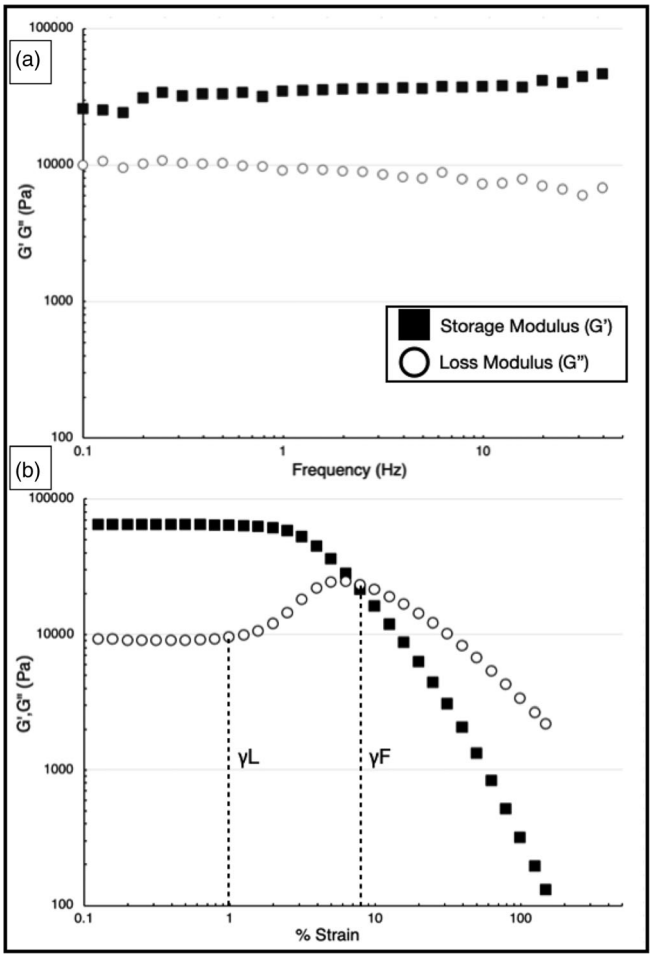

FIGURE 5 Rheological behavior of 50% F68-water mixture under (a) frequency sweep and (b) strain sweep

appearance data and also looking forward to future applications, the 50% F68-water composition looks the most promising in terms of handling and further processing for a drug delivery system. Therefore, this mixture composition was investigated in detail, first with a more in-depth rheological testing procedure, second with the particle size and morphology and finally a long-term stability study.

For the rheological measurements, the 50% F68-water mixture was examined using both a frequency sweep (0.1–50 Hz at 0.1% strain) and a strain sweep (0.1%–150% at 1 Hz). The results are presented in Figure 5(a) and show that during the frequency sweep that G′ > G" over the entire frequency range. This is a conventional trend for cubic phase systems[34–36] with the system defined as rubbery plateau. Under the frequency sweep test parameters, the crossover between G′ and G" was not observed in this study which is again conventional in gel-like systems. The strain sweep in Figure 5(b) was used to assess the extent of the linear viscoelastic region for the gel. The results indicate linear behavior up to approximately 1% strain (γL) before G" starts to rise. As strain increases a crossover between G′ and G" occurs at ~8% strain (γF), which is when the sample resembles a liquid-like response.

The particle size and morphology the 50% F68-water mixture was assessed and compared to GMO-based cubosomes. The resulting average particle size of diluted F68-based cubosomes was 178.7 ± 8.7 nm with a PDI of 0.5 ± 0.02. This particle size is in the same range was of those reported in the literature of GMO-based

cubosomes.[37–39] While the PDI value <0.7 indicates that the samples do not have a broad size distribution.[40] To further confirm the formation of cubic structures, the morphology was examined using FE-SEM, and the obtained photomicrographs of a 10× diluted 50% F68-water mixture are presented in Figure 6 at two magnifications 10,000× and 80,000×. The micrographs show that the prepared cubosomes are spherical in shape, with rough nodular surfaces which has been reported previously in cubosome systems,[41] the size of the particles is within the nano-size with the clusters confirming the results of DLS particle size measurements.

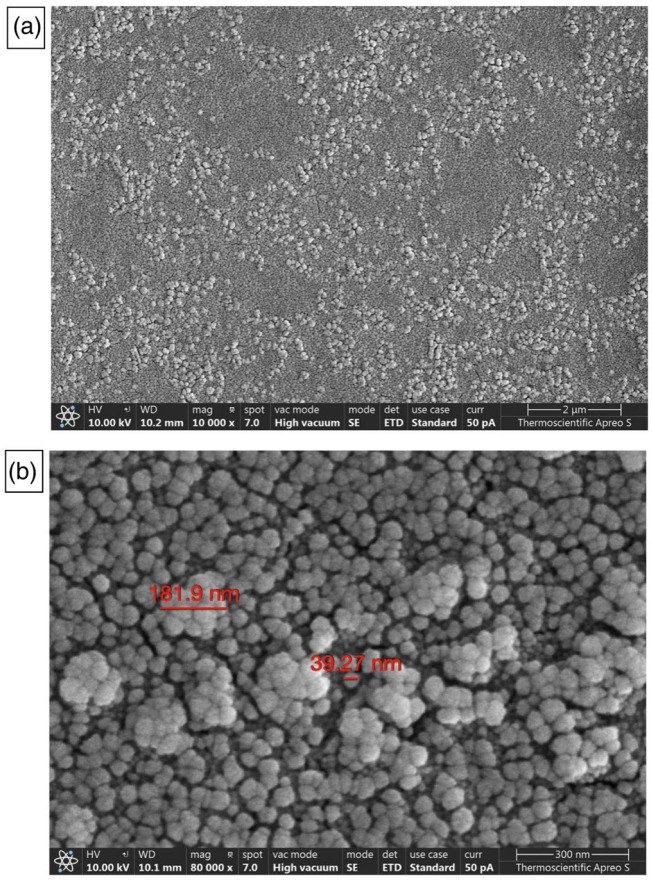

FIGURE 6 FE-SEM micrographs at magnifications of (a) 10,000× and (b) 80,000× of F-68 based cubosome dispersions 10X diluted [Color figure can be viewed at wileyonlinelibrary.com]

The next series of results looked at the stability of the 50% F68-water system. Although the internal mesophase of LLC particles are thermodynamically stable, cubosomes are often less colloidally stable than regular emulsions in an aqueous solution. Therefore, a steric stabilizer is required to retain colloidal stability.[42] By far the most widely and frequently used steric stabilizer for cubosomes is F127. In LLC dispersions, F127 acts as a steric stabilizer through the incorporation or adsorption of the hydrophobic PPO block onto the surface of the nanostructure. While the PPO domain/block acts as an "anchor" to the particle, the hydrophilic PEO chains extend to cover the surface, providing steric shielding and stabilizing the colloidal particles in the aqueous solution.[43] Due to F68 belonging to the same family as F127, a solely F68 system was investigated for long term stability. The stability of the Im3m F68-based cubosomes was studied for 10 months at ambient temperature. The cubosome particles appeared as a viscous gel without obvious aggregation. The 2D SAXS patterns and the 1D diffractograms are presented in Figure 7(a,b). The SAXS data showed diffraction peaks with relative position up to the fourth order at ratios of $\sqrt{2}:\sqrt{4}:\sqrt{6}:\sqrt{8}$. Comparing to the SAXS profiles of bulk cubic phase, three similar reflections ($\sqrt{2}:\sqrt{4}:\sqrt{6}$) of a primitive cubic lattice of the Im3m group space, were observed for samples aged 10 months. This clearly confirms that, the F68-based cubosomes are composed of a

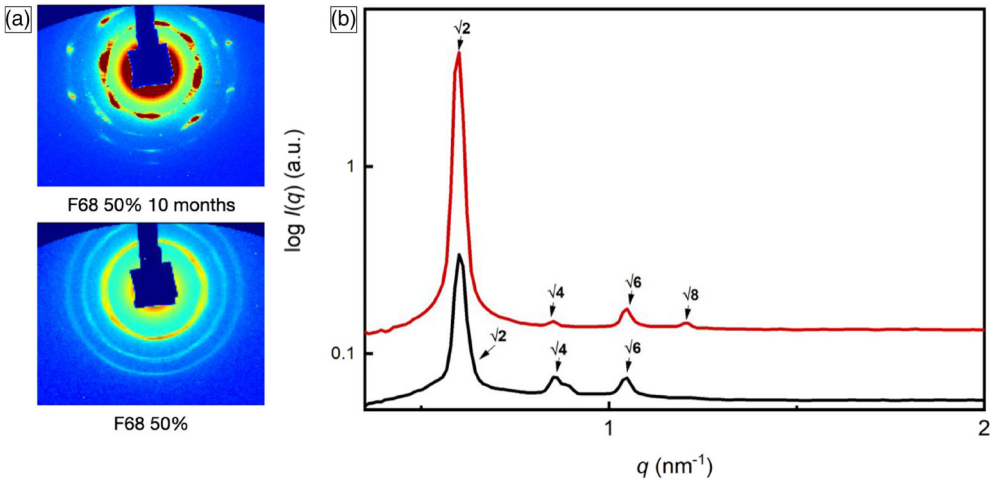

FIGURE 7 (a) 2D small angle X-ray scattering pattern for 50% F68-water cubosomes before (black) and after 10 months aging (red). (b) Small angle X-ray scattering diffractogram with Bragg peaks and peak assignment [Color figure can be viewed at wileyonlinelibrary.com]

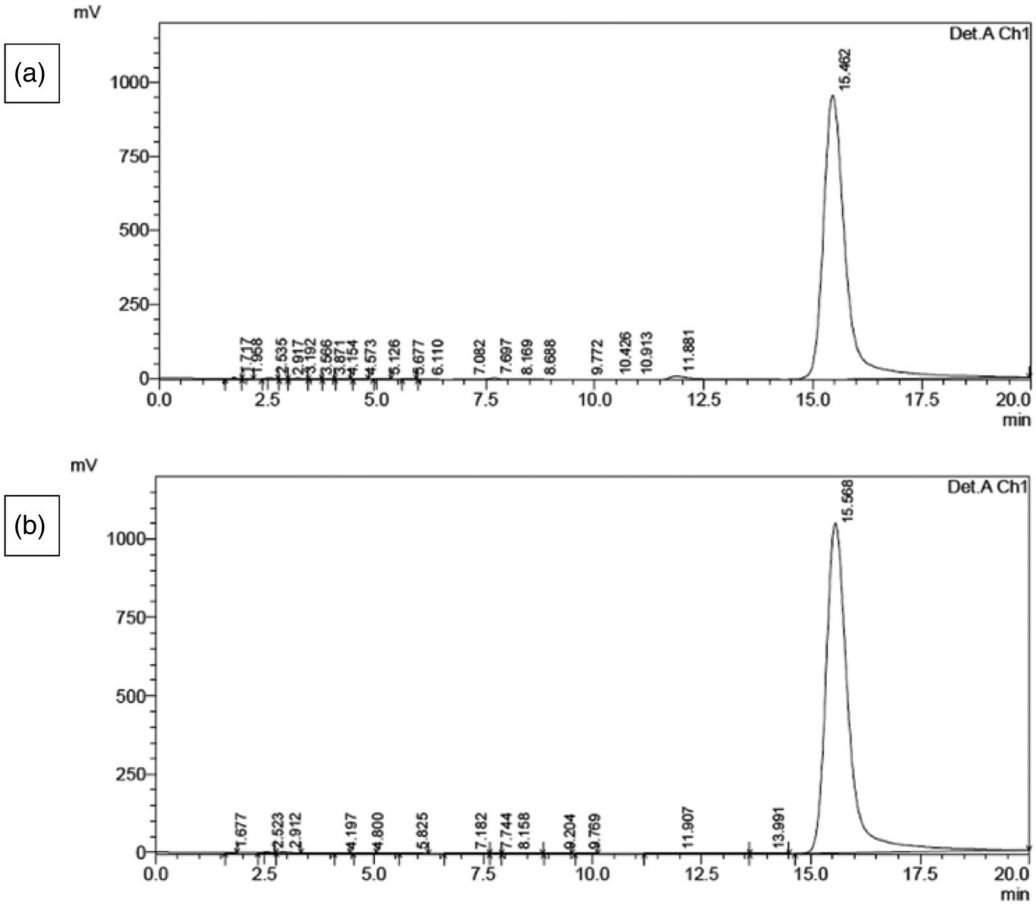

Substance	Retention Time	Area	Height	Area %
Standard AR	15.46	34584334	959866	96.84
AR enriched	15.57	37749356	1052528	99.25

FIGURE 8 Qualification of the AR-enriched extract (a) HPLC chromatogram of the standard AR, and (b) HPLC chromatogram of the AR-enriched extract with the corresponding HPLC data

thermodynamically stable system without the need of an additional stabilizing agent.

3.3 | Incorporation of AR extract loaded F68-based cubosomes

In the F68-based cubosomes, the hydrophobic chains form a lipid bilayer with a cubic phase, with the hydrophilic PEO moieties forming a water channel. Thus, poor water-soluble ingredients have the potential to be incorporated within this lipid bilayer (as shown in Figure 1). To test, this hypothesis, AR was added to the 50% F68-water cubosomes. First, the amount of AR in the exact was measured using HPLC and was found to be higher than 95% according to the HPLC calibration curve generated from the standard AR. The HPLC chromatograms and area% of the standard AR and AR enriched are shown in Figure 8. Therefore, confirming that the extract is a predominantly AR-enriched extract. When the AR extract was encapsulated in the cubosomes, the results show there is a 950-fold increase in the AR solubility compared with the solubility of AR water at 25°C of 2.6 μg/ml. The developed F68-based cubosome incorporated with 2.5% AR extract (the maximum AR-loaded concentration) were characterized using SAXS. The 2D SAXS patterns and the 1D diffractograms are presented in Figure 9(a,b). Peaks originating from the Im3m cubic

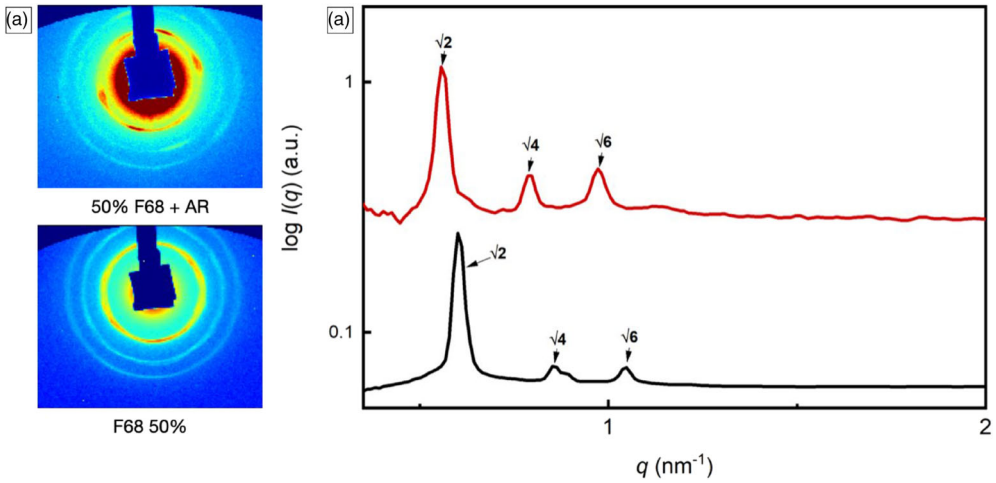

FIGURE 9 (a) 2D small angle X-ray scattering pattern for 50% F68-water cubosomes with AR (red) and without AR extract (black). (b) Small angle X-ray scattering diffractogram with Bragg peaks and peak assignment [Color figure can be viewed at wileyonlinelibrary.com]

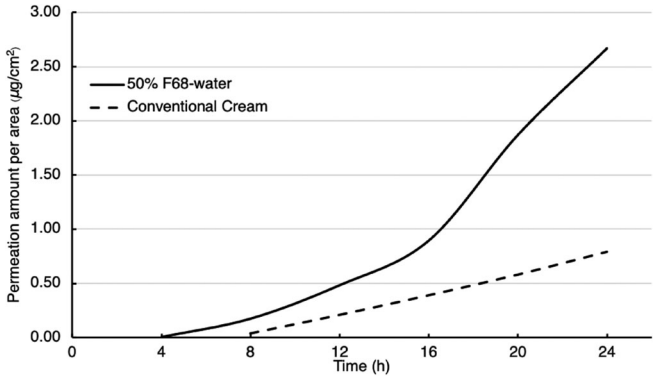

FIGURE 10 Permeation of AR from F68-based cubosome and conventional emulsion-based cream in phosphate buffer saline solution, pH 7.4

√2:√4:√6 became more prominent when 2.5% AR was incorporated. The prominence of the peaks maybe due to AR molecules interacting the cubosome, enhancing its structure rather than disrupting the internal structure.[44]

As presented in Figure 9, AR-loaded F68 based cubosomes were successfully developed. These systems are generally used for topical application and therefore, permeation is an important parameter to measure, to study the potential of the carrier system. The results of permeation experiment (Figure 10) show that the permeation of AR was linear with permeating time for F68-based cubosomes and cream. The AR loaded F68-based cubosome was not found in the receptor solution during the first 3 h but was found at 4 h, while in the AR-loaded conventional cream the AR was not found until 8 h. The AR permeation rates of cubosomes and cream at steady state (Js) obtained from the slope of the linear portion of the cumulative amount that permeated through the membrane per unit area versus time plot were calculated. F68-based cubosomes exhibited a much higher permeation rate (0.921 μg/cm^2) than the conventional cream (0.046 μg/cm^2). The permeation rate of AR loaded cubosomes was around 20-times faster than cream-based system, indicating the enhanced efficiency of cubosomes to improve the permeability of AR into skin as compared to a conventional cream system. The release pattern in the present study, is believed to occur by utilizing the inherent structural advantages present with in the rigid cubic structures. The rigid structure of Im3m cubic consist of six water channels,[45] and these channels allow rapid release of the active greater than emulsion based. Also, the cubic systems show a higher surface area, which leads to enhanced burst release.[46] Therefore, the burst release allows for an increase in the permeability of the cubosomes. Also, the concentration gradient between the polymeric matrix and medium was greater, which offers increased flux over the conventional cream formulation. Furthermore, F68 itself is known to positively interact with skin lipids and therefore, can act as a skin permeation enhancer.[47]

4 | CONCLUSIONS

This work studied the self-assembly of poloxamer 188 (Pluronic® F68), morphology, particle size, stability, rheological behavior and carrier properties. The results of visualization, rheology and SAXS, were all in agreement that that aqueous solutions of nonionic surfactant F68 could form soft and rigid gels that possessed LLC structures. The SAXS data also showed that Im3m cubic phases are formed over a certain concentration range (45%–60%), which remained stable as cubic structures for at least 10 months without additional stabilizing agent. Their thermodynamic stability

is thought to arise from steric shielding of the F68 itself which is similar to how F127 behaves in MO-cubosome systems. To assess the use with poor water-soluble molecules AR was studied, first, it was observed that the developed F68-based cubosome possessed enhanced AR solubility due to the high affinity of this type of molecule with the hydrophobic regions present in the cubic structure. Second, the AR loaded F68-based cubosome exhibited faster release and greater enhanced the active when compared to a conventional emulsion-based cream. This is attributed the Im3m structure providing numerous water channel, a high surface area and the enhanced skin permeation properties of F68 itself. Overall, these results demonstrate the F68-based cubosomes represent a promising active ingredient carrier for enhancing the solubility and permeability of poor water-soluble molecules, while, using a robust and inexpensive preparation technique.

ACKNOWLEDGMENTS

We thankfully acknowledge Research and Researchers for Industries Grants (RRI) (grant number PHD57I0030); Newton Fund PhD placement 2017/18 (application ID 351290033); and S&J International Enterprises Public Company Limited for the financial support to this study.

ORCID

Gareth Ross https://orcid.org/0000-0002-2340-9568

REFERENCES

[1] P. Hoogevest, X. Liu, A. Fahr, *Expert Opin. Drug Deliv.* **2011**, *8*(11), 1481.
[2] S. V. Jermain, C. Brough, R. O. Williams, *Int. J. Pharm.* **2018**, *535*(1–2), 379.
[3] S. Sareen, G. Mathew, L. Joseph, *Int. J. Pharm. Investig.* **2012**, *2*(1), 12.
[4] Y. Huang, S. Guy, *RSC Adv.* **2018**, *8*(13), 6978.
[5] A. Angelova, B. Angelov, R. Mutafchieva, S. Lesieur, P. Couvreur, *Acc. Chem. Res.* **2011**, *44*(2), 147.
[6] J. C. Shah, Y. Sadhale, D. M. Chilukuri, *Adv. Drug Deliv. Rev.* **2001**, *47*(2–3), 229.
[7] T. H. Nguyen, T. Hanley, C. J. H. Porter, I. Larson, B. J. Boyd, *J. Pharm. Pharmacol.* **2010**, *62*(7), 856.
[8] R. Baskaran, T. Madheswaran, P. Sundaramoorthy, H. M. Kim, B. K. Yoo, *Int. J. Nanomed.* **2014**, *9*(11), 3119.
[9] J. Lai, Y. Lu, Z. Yin, F. Hu, W. Wu, *Int. J. Nanomed.* **2010**, *5*(1), 13.
[10] T. E. Hartnett, K. Ladewig, A. J. O'Connor, P. G. Hartley, K. M. Mclean, *RSC Adv.* **2015**, *5*(34), 543.
[11] M. A. Ali, S. Noguchi, Y. Iwao, T. Oka, S. Itai, *Chem. Pharm. Bull.* **2016**, *64*(6), 577.
[12] Q. Luo, T. Lin, C. Y. Zhang, T. Zhu, L. Wang, Z. Ji, B. Jia, T. Ge, D. Peng, W. Chen, *Int. J. Pharm.* **2015**, *493*(1–2), 30.
[13] H. Wang, P. B. Zetterlund, C. Boyer, P. T. Spicer, *J. Colloid Interface Sci.* **2019**, *546*(15), 240.
[14] L. V. Fei, A. N. Zesheng, W. U. Peiyi, *Nat. Commun.* **2019**, *10*(1), 1397.
[15] R. Koynova, M. Caffrey, *Chem. Phys. Lipids* **2002**, *115*(1–2), 107.
[16] J. Y. T. Chong, X. Mulet, D. J. Keddie, L. J. Waddington, S. Mudie, *Soft Matter* **2014**, *10*(35), 6666.
[17] A. Pitto-Barry, N. Barry, *Polym. Chem.* **2014**, *5*(10), 3291.
[18] P. Alexandridis, T. A. Hatton, *Colloids Surf. A Physicochem. Eng. Asp.* **1995**, *96*(1–2), 1.
[19] G. Wanka, H. Hoffmann, W. Ulbricht, *Macromolecules* **1994**, *27*(15), 4145.
[20] M. J. Lawrence, *Chem. Soc. Rev.* **1994**, *23*(6), 417.
[21] A. Zubair, K. S. Pramod, H. W. Musarrat, *J. Appl. Pharm. Sci.* **2016**, *6*(9), 204.
[22] F. Muller, A. Salonen, O. Glatter, *J. Colloid Interface Sci.* **2010**, *324*(2), 392.
[23] J. Zhai, L. Waddington, T. J. Wooster, M. I. Aguilar, B. J. Boyd, *Langmuir* **2011**, *27*(24), 757.
[24] A. M. Bodratti, P. Alexandridis, *Expert Opin. Drug Deliv.* **2018**, *15*(11), 1085.
[25] K. M. Lin, C. H. Liu, H. Y. Tu, H. H. Ko, B. L. Wie, *Food Chem.* **2009**, *115*(2), 558.
[26] B. L. Wie, J. R. Wenig, P. H. Chiu, C. F. Hung, J. P. Wang, C. N. Lin, *J. Agric. Food Chem.* **2005**, *53*(10), 3867.
[27] N. Tiraravesit, P. Humbert, S. Robin, M. Tissot, C. Viennet, J. Viyoch, *Photochem. Photobiol.* **2017**, *93*(5), 1232.
[28] K. Itsarasook, K. Ingkaninan, J. Viyoch, *Biologia* **2014**, *69*(7), 943.
[29] K. Luangpraditkun, P. Charoensit, F. Grandmottet, C. Viennet, J. Viyoch, *Oxid. Med. Cell Longev.* **2020**, *2020*, 17.
[30] P. Alexandridis, U. Olsson, B. Lindman, *Langmuir* **1998**, *14*(10), 2627.
[31] N. Eblovi, S. Rasi, M. Drechsler, G. M. Di Gregorio, E. Menegatti, R. Cortesi, *AAPS PharmSci* **2003**, *5*(4), 62.
[32] L. Boge, K. Hallstensson, L. Ringstad, J. Johansson, T. Andersson, M. Davoudi, P. T. Larsson, M. Mahlapuu, J. Håkansson, M. Andersson, *Eur. J. Pharm. Biopharm.* **2019**, *134*, 60.
[33] T. Pitaksuteepong, A. Somsiri, N. Waranuch, *Eur. J. Pharm. Biopharm.* **2007**, *67*(3), 639.
[34] C. Speziale, R. Ghanbari, R. Mezzenga, *Langmuir* **2018**, *34*(17), 5052.
[35] R. Mezzenga, C. Meyer, C. Servais, A. I. Romoscanu, L. Sagalowicz, R. C. Hayward, *Langmuir* **2005**, *21*(8), 3322.
[36] M. Mendozza, L. Caselli, C. Montis, S. Orazzini, E. Carretti, P. Baglioni, D. Berti, *J. Colloid Interface Sci.* **2019**, *541*(1), 329.
[37] S. B. Rizwan, D. Assmus, A. Boehnke, T. Hanley, B. J. Boyd, T. Rades, S. Hook, *Eur. J. Pharm. Biopharm.* **2011**, *79*(1), 15.
[38] N. M. Morsi, G. A. Abdelbary, M. A. Ahmed, *Eur. J. Pharm. Biopharm.* **2014**, *86*, 178.
[39] Y. S. R. Elnaggar, S. M. Etman, D. A. Abdelmonsif, O. Y. Abdallah, *Int. J. Nanomedicine* **2015**, *27*(10), 5459.
[40] M. Danaei, M. Dehghankhold, S. Ataei, F. H. Davarani, R. Javanmard, A. Dokhani, S. Khorasani, M. R. Mozafari, *Pharmaceutics* **2018**, *10*(2), 57.
[41] S. B. Rizwan, Y. D. Dong, B. J. Boyd, T. Rades, S. Hook, *Micron* **2007**, *38*(5), 478.
[42] K. Larsson, *J. Chem. Phys.* **1989**, *93*(21), 7304.

[43] J. Y. T. Chong, X. Mulet, B. J. Boyd, C. J. Drummond, Steric stabilizers for cubic phase lyotropic liquid crystal nanodispersions (cubosomes). in *Advances in Planar Lipid Bilayers and Liposomes* (Eds: A. Igli'c, C. V. Kulkarni, M. Rappolt), Academic Press, Waltham, MA **2015**, p. 131.

[44] Z. Yang, X. Peng, Y. Tan, M. Chen, X. Zhu, M. Feng, *J. Nanomater.* **2011**, *7*, 23.

[45] R. Rajabalaya, M. N. Musa, N. Kifli, S. R. David, *Drug Des. Devel. Ther.* **2017**, *11*, 393.

[46] P. T. Spicer, *Curr. Opin. Colloid Interface Sci.* **2005**, *10*(5–6), 274.

[47] H. A. Benson, *Curr. Drug Deliv.* **2005**, *2*(1), 23.

How to cite this article: S. Yakaew, K. Luangpradikun, P. Phimnuan, N. Nuengchamnong, N. Kamonsutthipaijit, S. Rugmai, W. Nakyai, S. Ross, M. Ungsurungsei, J. Viyoch, G. Ross, *J. Appl. Polym. Sci.* **2021**, e51612. https://doi.org/10.1002/app.51612